ELEMENTS OF POSITRON PRODUCTION SCHEME FOR ILC
CORNELL PERSPECTIVE[1]

Alexander Mikhailichenko, LEPP, Ithaca, NY 14853

The scheme for positron production with helical undulator remains likely the only practical one. At first stage unpolarized positrons in quantities required can be generated with relatively short, ~20 m long undulator. Undulator with the length increased to ~120 m, can produce positrons with polarization ~70% level. With 250 m–long undulator polarization can reach ~85%. The way of positron production with undulator is preferable one as it yields fewer radioactivities and it is cheaper, than the one with traditional approach. Polarized electrons can be generated in this way also.

Described are the Cornell plans/visions for development of such a system.

INTRODUCTION

Let us remind the basic parameters in circulation now, which are important for positron production.

Number of particles per bunch	$N_b = 2\times10^{10}$
Number of bunches per train	n_b=2820 (5640)
Repetition rate	f=5 (10) Hz
Bunch sequence	~308 ns
Total train duty	~1ms
Positrons Target/IP	1.5

Thanks to the presence of starter source, positron wing of collider works independently from the electron one. Starter source (having the size of a barrel) generates low intensity, 1 MeV electrons which are accelerated in the main structure up to 0.5 GeV. *Electrons* directed then to the positron target, the same as for polarized positron production, where they are generating positrons, which are collected by the same optics. After the necessary amount is accumulated (stacked) in the damping ring, the beam from damping ring goes into main linac. After few cycles, the polarized positron beam becomes restored. Soft bend off acceleration line to the undulator axis made achromatic. Feedback system, operating on bunch to bunch basis, makes this scheme stable under charge fluctuation.

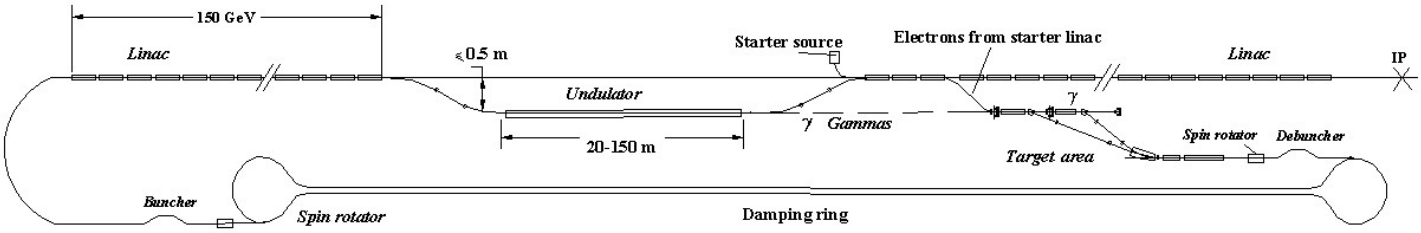

FIGURE 1: Positron wing of collider works independently from electron one, thanks to the presence of starter source.

[1] Electronic version is available at http://www.lns.cornell.edu/public/CBN/2005/CBN05-17/CBN05-17.pdf. Supported by NSF

To work at lower energy, giga Z, the beam decelerated in the residual part of accelerator. As the energy spread generated in undulator, is increased, during deceleration some losses of luminosity is possible. The undulator parameters in this regime of operation can be optimized, so the luminosity reduction is minimal. *Debuncher* before damping ring required as the bunch lengthening during collection might be not enough and the short bunch might be able to develop instabilities in a damping ring. Equilibrium bunch length in a damping ring is much longer, than in linac (remember bunchers at the linac entrance).
So we are paying attention to all elements: undulator, target, collection optics, preliminary acceleration right after the target, spin manipulation, injection optics down to damping ring and scheme of stabilization of current.

This way is also working for *polarized electrons production*.

Let us first calculate the power balance in the beams. The total number of photons in all spectrum radiated in undulator having *M* periods and undulatority factor *K* goes to be

$$N_g \cong \frac{4p}{3} a \cdot M \cdot \frac{K^2}{1+K^2}$$

For 100 m-long undulator with period $l \cong 1$ cm, $M=10^4$. For $K^2=0.15$ the last formula gives $N_g \cong 80$ photons. As the energy of each photon for primary beam energy $E \cong 150 GeV$ goes to be

$$E_{g\max}[MeV] \cong \frac{2.48 \cdot (g/10^5)^2}{l_u[cm](1+K^2)} \cong \frac{2.48 \cdot 9}{1.15} \cong 19.4,$$

then the total number of photons per bunch goes to be $N_{g\,bunch} \cong 80 \times 2 \cdot 10^{10} = 1.6 \cdot 10^{12}$ and the total energy carried by all the photons radiated by bunch goes to be

$$E_{g\,bunch} \cong N_{g\,bunch} \times E_{g\max} \cong \tfrac{1}{2} \times 1.6 \cdot 10^{12} \times 19.4 \cdot 10^6 \times 1.602 \cdot 10^{-19} \cong \tfrac{1}{2} \times 1.74 \times 1.94 \times 1.6 = 2.5[J].$$

where factor ½ takes into account that the half of the photons carry this energy. Train will radiate

$$E_{g\,bunch} \cong N_{g\,bunch} \times E_{g\max} \times n_b \cong E_{g\,bunch} \times n_b = 2.5 \times 2820 = 7644\ [J] \cong 7kJ,$$

and the energy carried by all photons radiated per second will be $E_{g\,tot} \cong 35kJ$. The power carried by these photons goes to be $P \cong 35\ kW$. For 20 MeV gammas approximately 13% of gammas deposited theirs energy in the target, brining the power deposited in the target to $P_{target} \cong 4.55$ kW.

So the average energy deposited in the target is not high, but the pulsed energy deposition makes the target problem severe, however.

Activities at Cornell cover undulator itself, bypass optics for main beam, target, collection optics, pre-accelerator, combining schemes, spin rotators and elements of channel up to the damping ring.

UNDULATOR

Activity in this field is covering the modeling of fringe fields, fabrication and test of prototypes, modeling technology.

Fringe fields compensation. This is the mostly important item for the scheme, if undulator installed before IP. Methods of compensation include proper tapering and installation the sections in series with alternative polarities. Tiny vertical emittance puts the limit for the field imperfections.

Cost estimation will be done after the first real scale prototype will be manufactured.

Test of module with beam at low energy can be done at Cornell. Some other Laboratories have abilities for such test also.

Perturbation of emittance is a crucial moment of all method, if undulator installed before IP.
2 m—long sections with the same spatial orientation of input and output ends installed in series and feed with opposite polarity. This automatically delivers first integral

$$I^1_{x,y} = \int_{-\infty}^{+\infty} H_{x,y}(s)ds = 0.$$

This integral is responsible for transverse kick, as $x' = I^1_x/(HR)$, $y' = I^1_y/(HR)$. So the 4m—long module delivers zero kick. To eliminate displacement, two 4 m–long modules need to be feed with opposite polarity. This will bring second integral to zero $I^{(2)}_{x,y} = \int_{-\infty}^{+\infty} ds \int_{-\infty}^{o} H_{x,y}(s)ds$ So two 4 m –long sections deliver zero first and second integral.

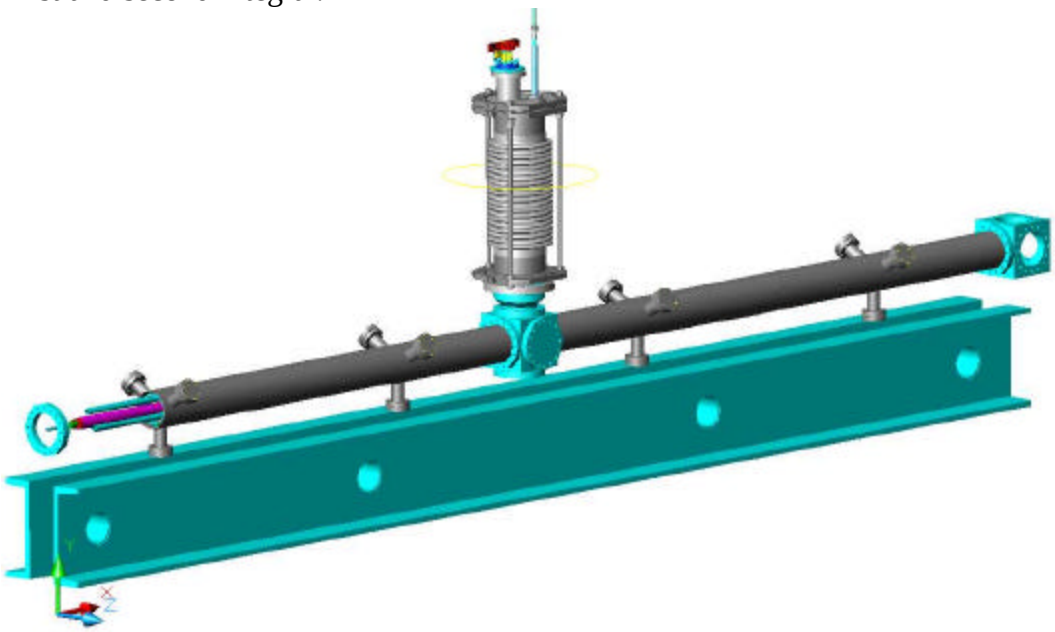

FIGURE 2: Cryomodule, 4 m—long. Cryostat contains two 2 m–long identical sections having opposite polarity. This delivers zero first integral along this module.

Correction elements include trim coils allowing generating dipole field in two rectangular directions located at the ends of each module. Natural realization of these trim magnets as having superconducting wiring and integrating into cryo-system.

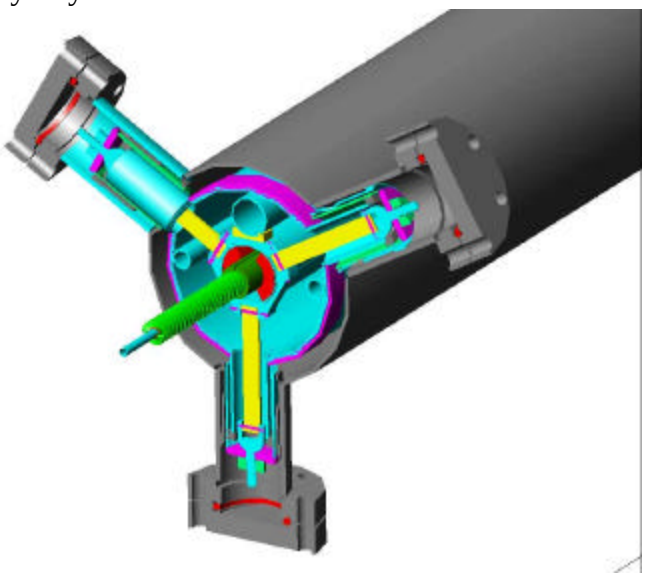

FIGURE 3: Details of cold mass support. Outer tube diameter is 5 inch.

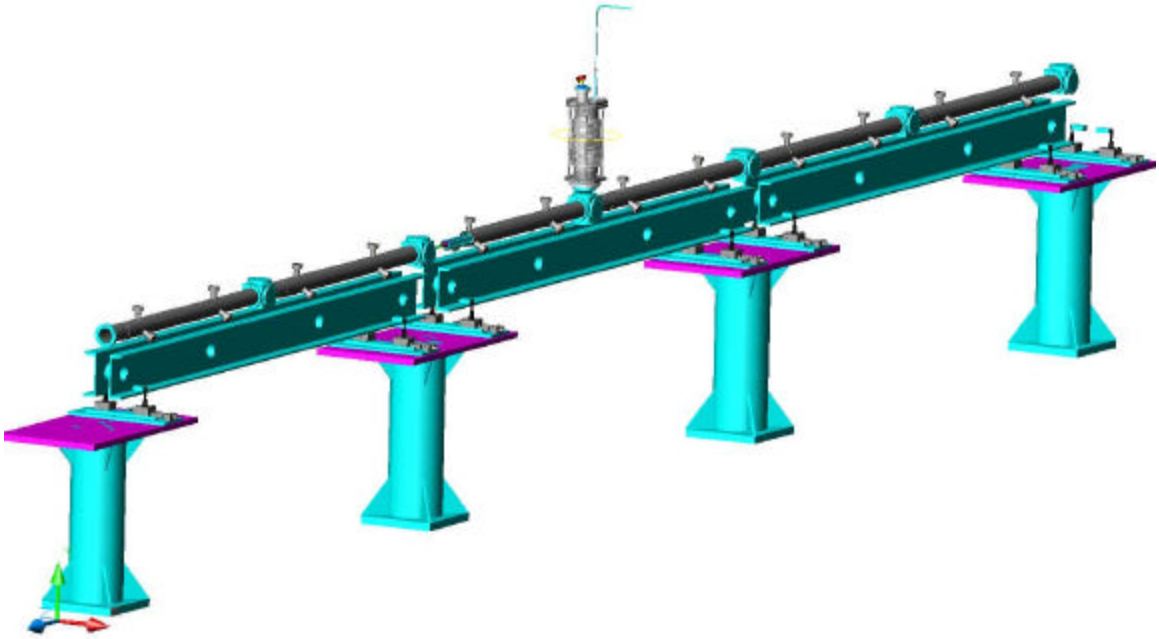

FIGURE 4: Sections installed in series.

Influence of the field roll-off in undulator

Inside undulator particles developing tiny helixes, having pitch angle $a \sim K/g$, and the radius of helixes is $a @ \lambda\!\!\!^{-}_u K/g$, where $\lambda\!\!\!^{-}_u = l_u / 2p$, l_u stands for period of undulator; we will be interested in $l_u \cong 1\ cm$. The numbers for angular spread and radius of helix for E=150 GeV ($g @ 3 \times 10^5$), and K~1 coming to $a \sim 3 \times 10^{-6}$ rad and $a \cong 10^{-5}/6p \cong 5 \cdot 10^{-7} cm$ respectively.

Meanwhile natural vertical angular spread inside the beam and the beam size $y\!\!\!^{\prime} @ \sqrt{ge_z / bg}$ and $\sqrt{\langle y^2 \rangle} \cong \sqrt{ge_y b/g}$, for invariant vertical emittance $ge_z @ 2 \times 10^{-8} m \times rad$ and the envelope function value $b @ 100m$, go to be

$$y\!\!\!^{\prime} @ \sqrt{2 \times 10^{-8}/3 \times 10^5/100} @ 2.6 \times 10^{-8} \text{ rad and } \sqrt{\langle y^2 \rangle} \cong \sqrt{2 \cdot 10^{-8} \cdot 100/3 \cdot 10^5} \cong 2.6 \cdot 10^{-4} [cm]$$

respectively. For horizontal motion, $ge_x \cong 2 \cdot 10^{-6} m \cdot rad$ giving all numbers ten times bigger.

Angular spread in radiation	$a \sim K/g$	3×10^{-6} (K=1)
Angular spread in beam, vert.	$y\!\!\!^{\prime} @ \sqrt{ge_z / bg}$	2.6×10^{-8}
Radius of helix	$a @ \lambda\!\!\!^{-}_u K/g$	$5 \times 10^{-7} cm$ (K=1)
Beam size, vertical	$\sqrt{\langle y^2 \rangle} \cong \sqrt{ge_y b/g}$	$2.6 \cdot 10^{-4} cm$
Beam size, radial	$\sqrt{\langle x^2 \rangle} \cong \sqrt{ge_x b/g}$	$2.6 \cdot 10^{-3} cm$

One can see that angular wiggling is much bigger, than natural angular spread in the beam. Meanwhile radiuses of helixes are much smaller, than the beam size. First fact makes possible angular separation for

reduction of contest of second harmonic and enhancing average polarization as it becomes reversed under angle $\sim 1/g$. *Important thing here is that the power falling on the target is reduced also by the same procedure (angular selection).*

All particles in cross-section are developing helixes with the same phase inside undulator, despite field dependence across aperture. The last generates ellipticity in helix. The field roll-off from the center of undulator, described in polar coordinates, is proportional to the square transverse radial displacement r

$$H_j(r,j,z) \cong H_0 \times \cos(j - j_0 - \frac{z}{\lambda\!\!\!^{-}_u}) \times \left[1 + \frac{1}{8}\left(\frac{r}{\lambda\!\!\!^{-}_u}\right)^2 + \frac{1}{768}\left(\frac{r}{\lambda\!\!\!^{-}_u}\right)^4 + \ldots\right],$$

where $H_0 \propto I/\lambda\!\!\!^{-}_u$ is the field at the axis, I stands for the current running in helix [CBN 02-10]. So in our case the second term for the particles at the distance $\sqrt{\langle x^2 \rangle} \cong 26 \cdot 10^{-4} cm$ goes to be

$$\frac{1}{8}\left(\frac{r}{\lambda\!\!\!^{-}_u}\right)^2 \cong \frac{\langle x^2 \rangle}{8\lambda\!\!\!^{-2}_u} \cong 3.3 \cdot 10^{-5}, \qquad \frac{\langle y^2 \rangle}{8\lambda\!\!\!^{-2}_u} \cong 3.3 \cdot 10^{-7}.$$

This means, that ellipticity is negligible, however. Important is that the difference in kicks obtained by the particles across the beam size will be different in the same proportion, if the helix is ended suddenly. As the field along the particle's trajectory oscillating, the nonlinear kicks are oscillating too. So resulting kick averaged along period will be different in accordance with formula, where for radius the value $r \cong \lambda\!\!\!^{-}_u K/g$ needs to be substituted now. In this case

$$\frac{1}{8}\left(\frac{a}{\lambda\!\!\!^{-}_u}\right)^2 \cong \frac{K^2}{8g^2} \cong \frac{0.15}{8 \cdot 9 \cdot 10^{10}} \cong 2 \cdot 10^{-13},$$

so the resulting angle after one period will be

$$\Delta x' \cong H_0 \times \frac{K^2}{8g^2}\frac{l_u}{(HR)} \cong 0.4[T] \times 2 \cdot 10^{-13} \frac{1[cm]}{5 \cdot 10^4 [T \cdot cm]} \cong 0.16 \times 10^{-17} rad.$$

where magnetic rigidity of particle at 150 GeV was substituted $(HR) = 5 \cdot 10^4 [T \cdot cm]$ and H_0=0.4 T. After all M=10^4 periods the angle goes to be $\Delta x' \cong 0.16 \times 10^{-16} rad \times 10^4 \cong 1.6 \cdot 10^{-13} rad$.

Focusing in undulator can be evaluated as the following. The integral of gradient field due to passage over one period is

$$\int G ds \cong H_0 K / g .$$

So the focal distance of the whole undulator helix will be

$$F \cong \frac{(HR)}{M \int G ds} \cong \frac{(HR)}{M H_0 K} g \cong \frac{5 \cdot 10^4}{10^4 0.4 \times 0.4} 3 \cdot 10^5 [cm] = 10^7 [cm].$$

What important here is that the plane of magnetic field can be well controlled.

So finalizing one can say that the beam size is so small, that the difference in transverse kicks across the beam is small and perturbation of emittance is small too. Even so, the back up solution was here: to work in positron wing with doubled frequency and use one pulse just for positron generation, not for further acceleration. Fortunately this is not required.

This however is the mostly important subject for concern while attempting installation of undulator before IP.

COMBINING SCHEME

Attenuation coefficient $k \approx \exp(-\frac{1}{3}\frac{7}{9}t)$ for $t \gg 0.5$ (i.e. half radiation length) is around 0.87 i.e. only 13% of photons are lost. So it is possible to install second target and collect positrons independently from this second target. Combining could be arranged easily in the same separatrix of damping ring RF. Additional feed back system will be required for fast dump of coherent motion.

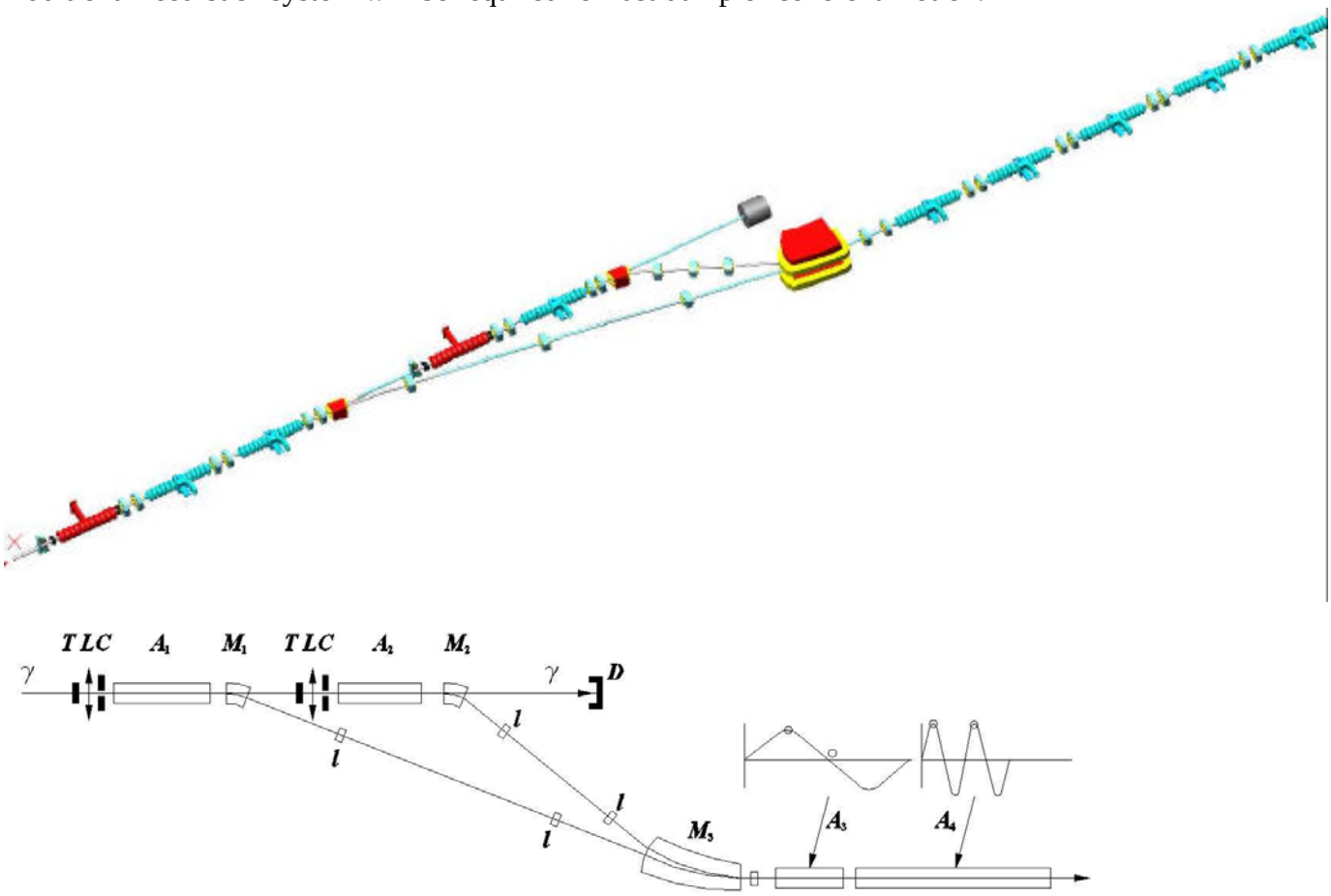

FIGURE 5: Combining scheme. Energy provided by acceleration structures A_1 and A_2 are slightly different, $A_1 > A_2$.

Here the gammas from undulator are coming from the left side and illuminate the target *T*. The short focusing lens *L* collects the particles and adjusts for further optics. Collimator *C*, located in front of accelerating structure cuts the particles with large transverse angle. By doing this it also cuts particles with low moments as this particles over-focused by lens *L*. An acceleration section A_1 delivers energy E_1 for the secondary beam. This beam of positrons is bending with the help of magnet M_1. The magnet M_1 and a part of the magnet M_3 with quadrupoles *l*, make an achromatic parallel shift of the positron beam. The second acceleration section A_2, delivers lower energy $-E_2$ to the beam, collected from the *second* target. The magnet M_2 with the part of the magnet M_3 and lenses, adjusted for achromatic parallel shift of the beam with the energy E_2. The difference in the path lengths of these two lines is an integer and a half of the wavelength in structure A_3. So the first sections in A_3 eliminate the energy difference. *D* is the gamma beam dump. Structure A_4 accelerates both bunches to the operational energy of the damping ring.

As the process of positron creation is axisymmetrical as well as short focusing optics is axisymmetrical too, the combining can be arranged in vertical plane for fitting in the tunnel if necessary. In this case all magnets: M_1, M_2, M_3 bend in vertical direction. Any arbitrary angle allowed as well.
Suggested average energy for the first structure A_1 is E_1=215 ± 5 *MeV* and for the second structure E_2 =175 ± 5*MeV*.

After energy is equalized two bunches can be stacked in the same separatrix. Feedback dumps coherent motion of centroids.

This combining can help in reduction of power deposition in target if each target made thinner, than optimal.

COLLECTION OPTICS

In part collection optics is under the test at E-166, where short period focusing lens is a part of collection optics.

$$F = \frac{4 \cdot (HR)^2}{\int H^2 ds}$$

For estimations, 10 MeV positrons /electrons have

$$(HR) = pc/300 = \frac{10 \cdot 10^6}{300}[G \cdot cm] = \frac{10 \cdot 10^3}{300}[kG \cdot cm] \cong 33 kG \cdot cm$$

so for longitudinal axis field ~20 kG and continuity 3cm,

$$F = \frac{4 \cdot (HR)^2}{\int H^2 ds} = \frac{4 \cdot 33 \cdot 33}{20 \cdot 20 \cdot 3} \cong 3cm$$

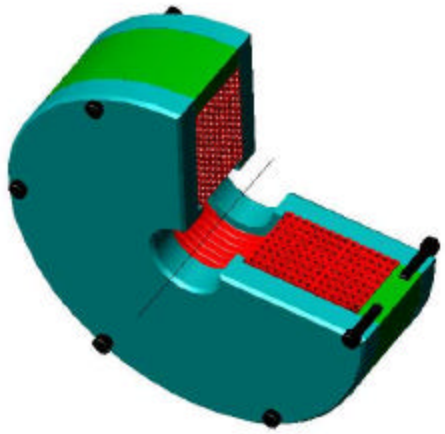

FIGURE 6: Cross section of E-166 short focusing lens.

This is a multi–turn lens wounded with hollow copper conductor having rectangular cross–section. Current density reaches ~45 A/mm^2.

This lens can be considered as a prototype for ILC one. Quasi—stationary feeding allows increase current up to 100 A/mm^2. This is possible taking into account that ILC beam lasts for ~1ms and repetition rate is 5 Hz only. So this lens can be feed with~ 5ms top flat current, arranged with the help of third harmonics. Thyristors can be used here adequately. Some parts of yoke can be made with laminations.

More fundamental solution is a SC lens.

For this lens we have choose the type with cold iron. The role of Iron important at lower field, however. Absence of iron allows reduction of the energy deposition by particles scattered from target.

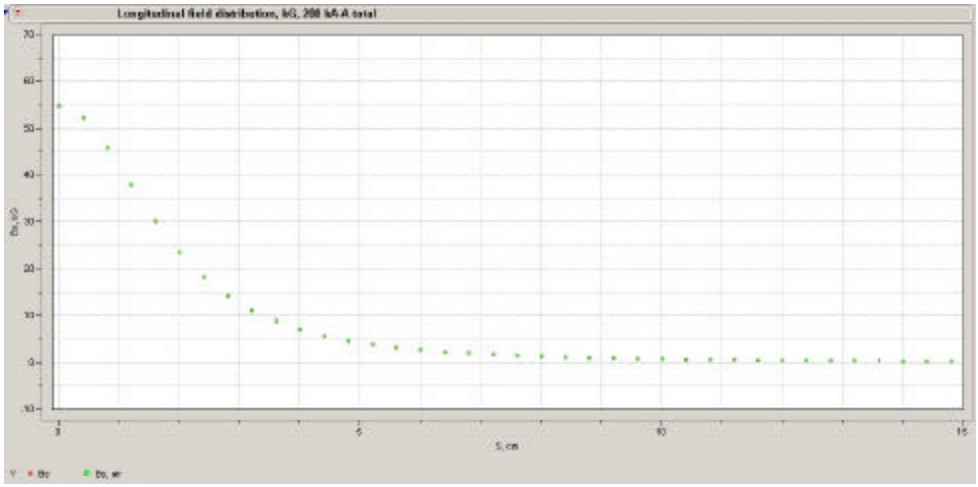

FIGURE 7: Input from iron is small at this field level.

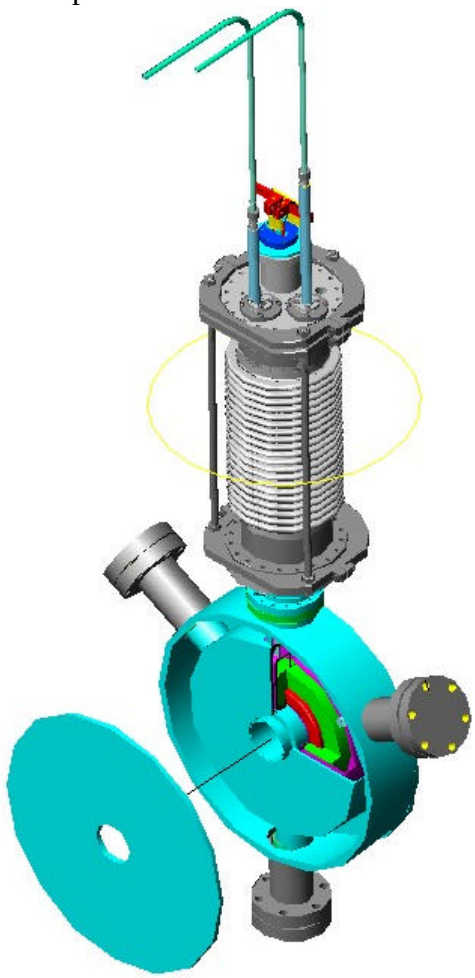

FIGURE 8: SC solenoidal lens.

This SC solenoidal lens uses the cold iron concept. However the Iron can be excluded as it can be seen from Fig.7. All vacuum chamber and cold mass container made from Al for reduction of isotopes accumulation.

TARGET

Shape of target.

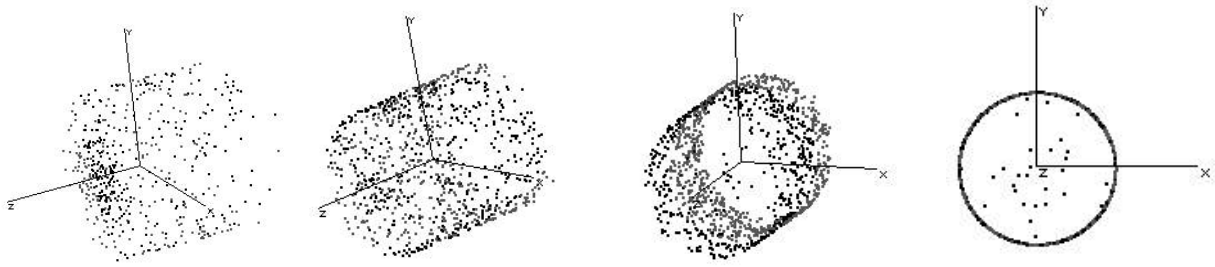

Short target | Longer target | Very long target | Very long target, front view

FIGURE 9: Different type of arrays of output coordinates. For the very long target, particles escape through the sidewalls mostly. Lengths of cylinders are not in scale with diameter.

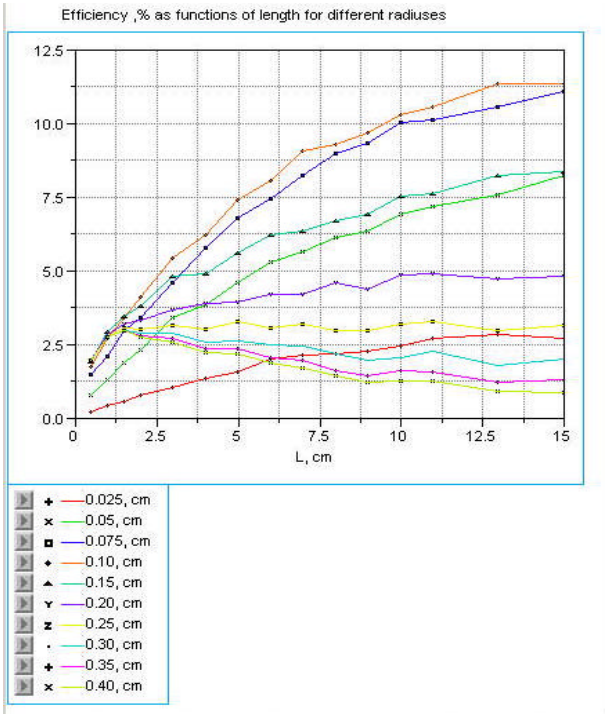

FIGURE 10: Efficiency as functions of target length for different values of radius.

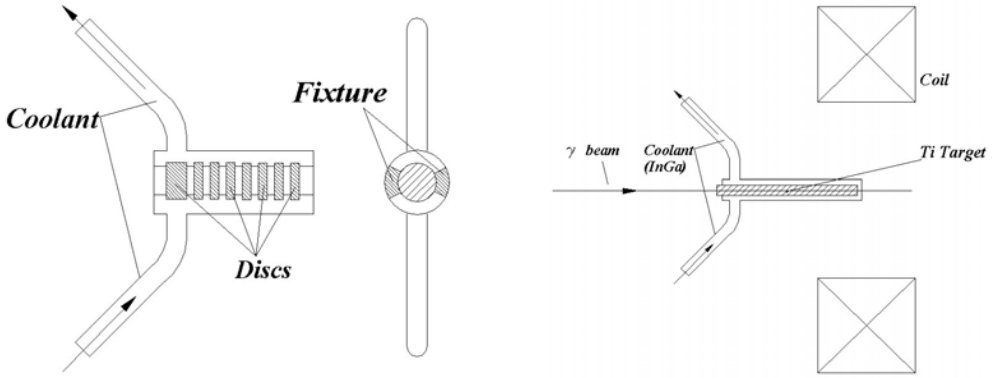

FIGURE 11: Sandwich-type high power target. W or Ti discs enclosed in Ti container with InGa coolant. At the right-long Ti target cooled by InGa coolant.

Let us say here without much consideration, that a suspension of W powder in liquid Li or InGa mixture can be considered as extreme media for target.

Utilization of few targets and combining positrons into longitudinal phase–space is also some kind of form-factor problem. One can reduce the thickness of the target to reduce the heating.

Although the rotating Titanium target satisfies requirements, we are looking around for supplementary engineering schemes, however. One of these is a liquid target.

Liquid metal target

High Z metals could be used here are the Lead, Mercury. InGa alloy also can be used here if filled with W powder.

Mercury has X_0 =4.8 mm, density $r \cong 13.6$ g/cm^3, heat capacity $C \cong 0.14 J/cm^3/^oK$, boiling temperature T_b=356.58^{o}C . Let us take for estimations the average power deposition ~5 kW. So every second Q=5kJ is deposited in a target. Let the Mercury jet has velocity ?=10m/sec and dimensions S=1×0.24 cm^2 in cross section. So the volume passed per second goes to be $V \cong 240 cm^3$. Due to turbulence all energy deposited evenly. The temperature gain goes to be

$$\Delta T \cong \frac{Q}{rVC} \cong \frac{5000}{12.6 \cdot 240 \cdot 0.14} \cong 12^o\text{C},$$

So from the point of average power deposition everything is acceptable.

Target unit is shown in Fig. 12. Here Mercury at conversion point is running in the channel with rectangular cross-section in profiled Titanium duct. At the bottom of extension there is the Mercury surface as the flow is interrupted by profiled extension.

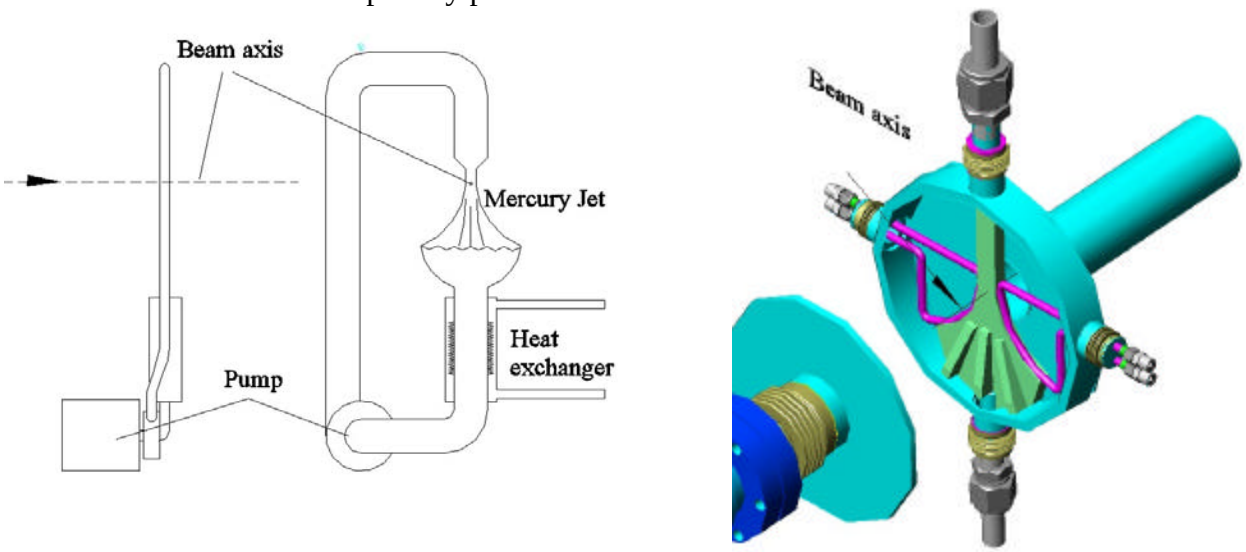

FIGURE 12: Scheme of liquid target, left. 3D view of the jet chamber is represented at the right. Diameter of the chamber is ~10 cm.

For $t \cong$ 300 nsec the jet will pass $L \cong vt = 10 m/\sec \times 300 \cdot 10^{-9} = 3 \cdot 10^{-6} m = 3 mm$ only, but for the time while the train passes, the distance will be $L \cong vt = 10 m/\sec \times 10^{-3} = 10 \cdot 10^{-3} m = 1 cm$. Energy deposited in the target *by one train* will be

$$Q_{train} = \frac{Q}{f} \cong \frac{5 \cdot 10^3}{5} \cong 1000 J$$

in a volume $V \cong LS \cong 1cm \times 1 \times 0.24 = 0.24cm^3$, so for the temperature gain $\Delta T \cong 320^o C$ (starting from T=37^{0}C) the energy absorbed will be

$$Q \cong rVC\Delta T \cong 12.6 \times 0.24 \times 0.14 \times 320 = 135\ [J]$$

While becoming a vapor, the latent heat of vaporization needs to be applied to the liquid. Specific latent heat of vaporization for Mercury at 357 ^{o}C is C_L=294*J/g*, so the energy absorbed by volume V=0.24cm^3 will be

$$Q_L \cong rVC_L \cong 12.6 \times 0.24 \times 294 = 890J$$

So the total energy absorbed by this volume will be

$$Q_{tot} \cong 890+135=1025[J]$$

This number means that Mercury *will remain liquid* at boiling temperature, however. Thus the droplets condensed at the bottom metal surface. Looks like the mass depletion effect needs to be taken into account. The mixture of vapor and drops hit the mercury surface. The liquid surface accepts the shocks from droplets. So, this target is able to absorb ~5 kW under parameters specified.

Remember, the speed of Mercury jet was taken 10 m/s only. For velocity of jet

$$v \cong \sqrt{\frac{P}{r}},$$

where P stands for pressure at the entrance of jet chamber. For moderate pressure P=30kg/cm^2 (30 atm), one can expect the velocity 21m/s. So that is the real resource here. We would like to say, that the Mercury flow in other, than jet chamber is slow due to extended diameter of tubes.

Accelerating structure right after the target and collection system more likely is a copper conducting one immersed in solenoidal field. The following structure(s) might be SC ones. However, as in front of structure there is a collimator, the first structure also can be a SC one. Additional focusing can be arranged with the help of irises having elliptical passing holes. Orientation of axes of these ellipses at opposite sides of cavities turned with 90 degrees.

COLLIMATOR

The primary electron beam with energy E_0, when hits the target, develops a cascade, what is a mixture of electrons, positrons and gammas. Namely these gammas are responsible for positron creation in electric field of nucleus of target material. This cascade develops along the target starting from the points of penetration of initial beam. The cascade propagates inside matter until energy of particles reaches the critical value, $E_c \approx 610/(Z+1.24)$, MeV; Z stands for atomic number. Transverse size of the cascade in maximum is of the order of Molière radius $R_M \approx X_0 E_s / E_c$, where X_0 is a radiation length, $E_s = \sqrt{4p/a} \cdot mc^2 \cong 21.2MeV$ –is a scale energy. Naturally, the Molière radius, expressed in cm, is bigger for lighter materials, as $R_M \approx 0.035 \times Z \times X_0$ and $X_0 \propto A/Z^2$, so $R_M \propto A/Z$, where A is atomic weight. For W with its Z=74, $R_M^W \approx 2.57X_0$ ($l_M^W = 0.9$cm), as geometrical length corresponding to the radiation one is $l_{X_0} \approx 0.35cm$. For Ti, with its Z=22, $R_M^{Ti} \approx 0.7X_0$ ($l_M^{Ti} = 2.45$cm), as $l_{X_0} \approx 3.55cm$. Cascade reaches its maximum at the depth $t_{max} \approx X_0 \ln(E_0/E_c)/\ln 2$ with the number of the particles there about $N_{max} \approx E_0/E_c$. So one can estimate geometrical volume occupied by cascade as

$$V_c \approx \frac{\pi}{3} l_{t_{max}} l_M^2 \approx \frac{\pi}{3 \ln 2} l_{X_0}^3 \left(\frac{E_s}{E_c} \right)^2 \ln \frac{E_0}{E_c} \propto l_{X_0}^3 \cdot Z^2 \propto A^3 / Z^4 \ .$$

The ratio of these volumes for Tungsten and for Titanium goes to be $V_c^{Ti} / V_c^{W} \propto \left(\frac{l_{X_0}^{Ti}}{l_{X_0}^{W}} \right)^3 \times \left(\frac{Z^{Ti}}{Z^{W}} \right)^2 = \left(\frac{3.55}{0.35} \right)^3 \times \left(\frac{22}{74} \right)^2 \approx 88$, i.e. the volume involved in cascade inside Ti is about 88 times the volume inside W for the same initial energy of primary electrons. The number of particles in cascade for W will be ~3.4 times bigger than in Ti. Of course, this is estimation only, and gives qualitative numbers; accurate calculation needs to be carried numerically.
So depending on the task, the transverse size of collimator can reach couple Molière radiuses.

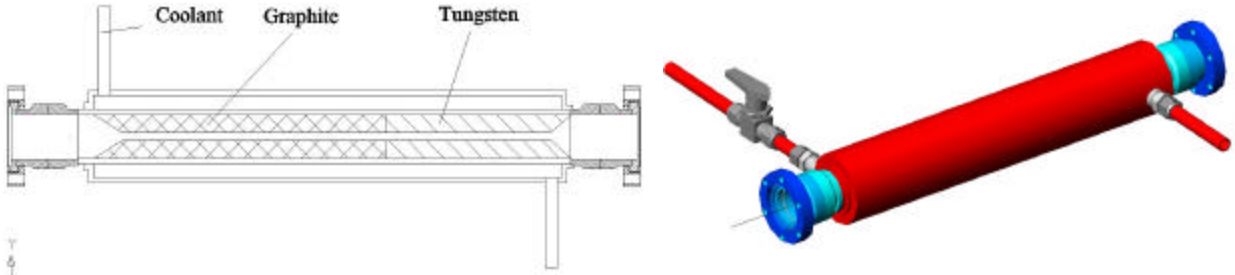

FIGURE 13: Collimator with Graphite. Flanges are 2 ¾ inch in diameter.

Pyrolytic Graphite (PG) is used here. The purpose of it is to increase the beam diameter, before entering to the W part. Vacuum outgassing is negligible for this material. Heat conductivity ~300 W/m-^{o}K is comparable with meals. *Beryllium* is also possible here, depending on task.
Other example is a *collimator with rotating liquid*.

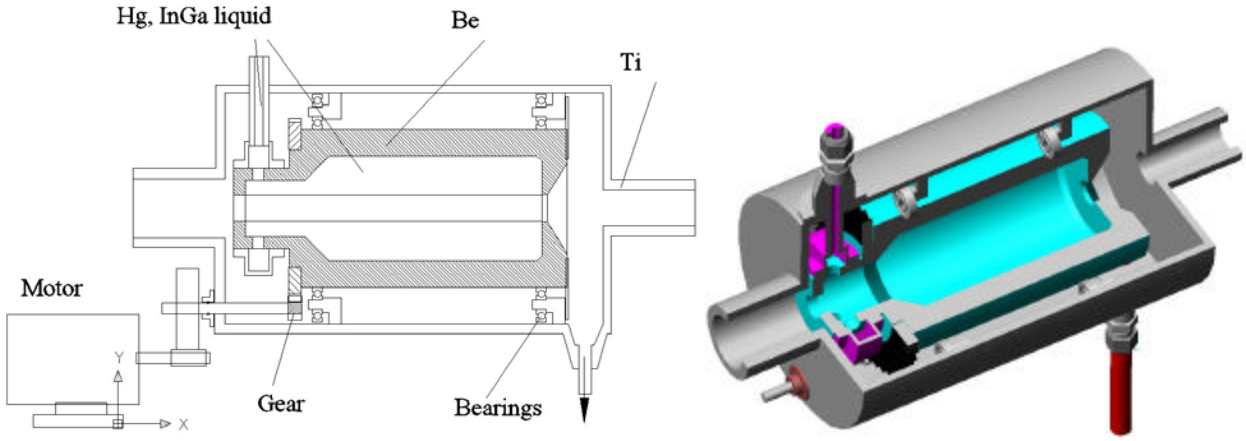

FIGURE 14: High average power collimator. Beam is coming from the right.

To fill the inner volume, the cylinder and liquid must have angular speed $w \geq \sqrt{g / r}$, where g=9.8m/s^2, and r stands for the inner radius. Let us take for estimations r =2mm=0.002 m, then $w \geq \sqrt{9800 / 2}$ =70 rad/s or 11 turns/s. The last number looks reasonable.
In the Figure 14, at the right side, the diameter of the hole in bottom of Be cylinder is smaller, than at the left side.

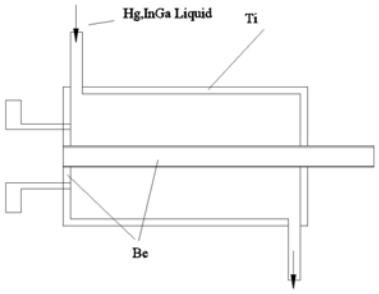

FIGURE 15: Simplified concept of liquid metal collimator of Type II.

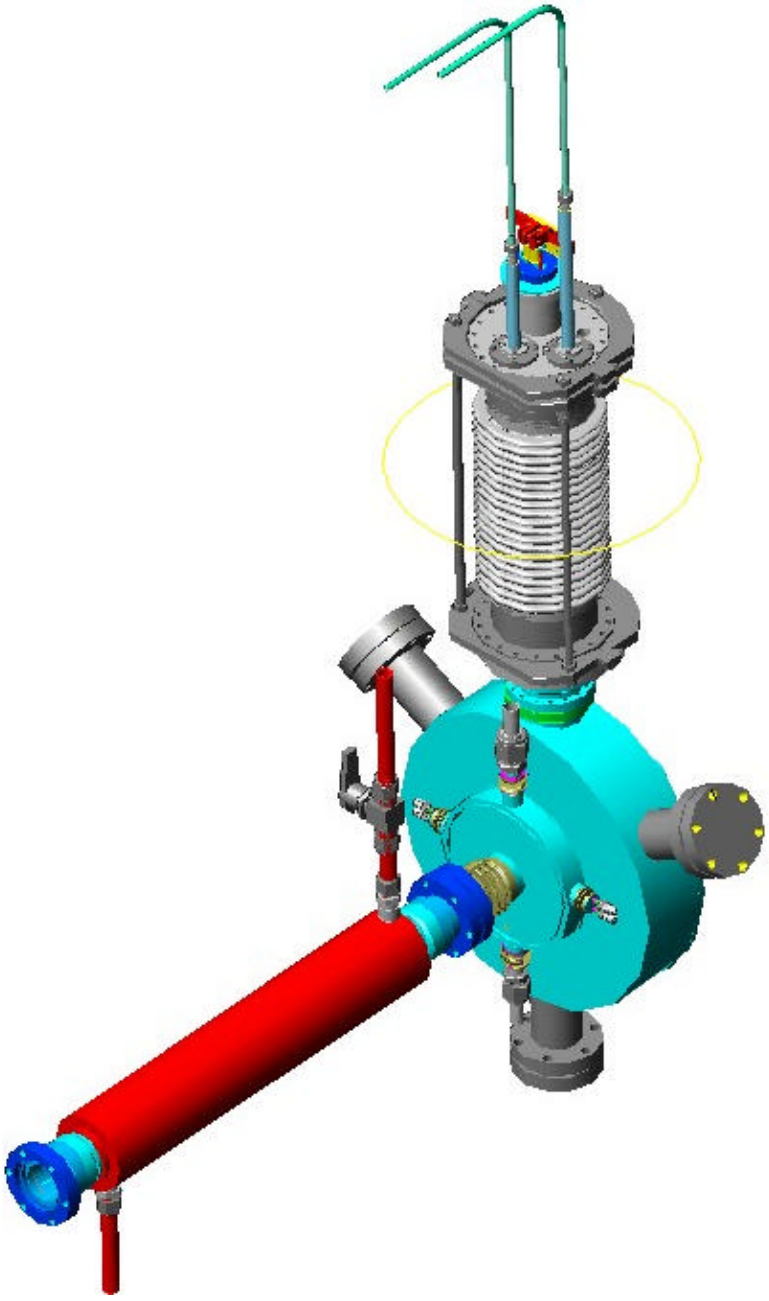

FIGURE 16: Conversion module. Flange shown is a 2¾ inch.

PRESENT ACTIVITY AT CORNELL

Perturbation of emittance in undulator is a key issue and calculation are rechecked. Simulation of different entrance tapering is under progress. Restoration of "start to finish" simulation code is under progress. It was written for Li lens as a focusing element.
Tested 30-cm long, 1 cm period undulator. Will be manufactured the new ones with improved tapering and winding.

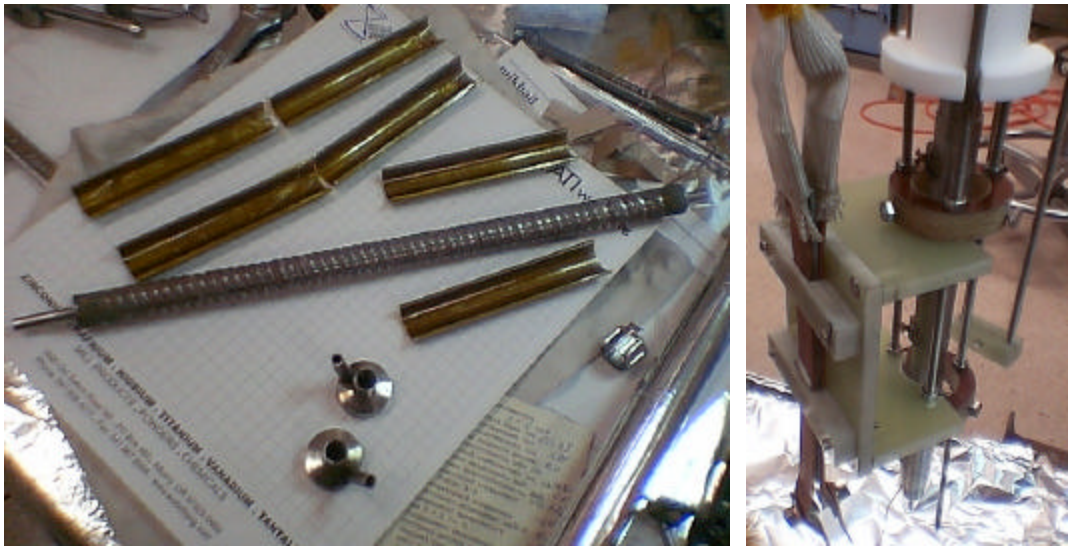

FIGURE 17: Cold mass test.

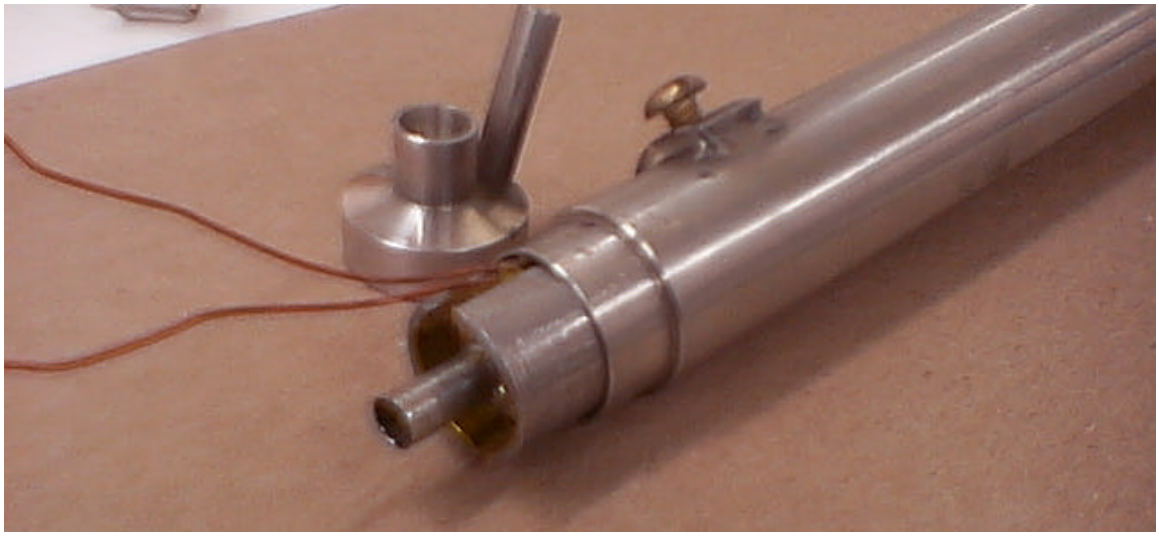

FIGURE 18: Undulator having period 10 mm and aperture 6mm develops $K \cong 0.33$ for I=200A. Tube diameter is 6 mm. Tested up to 400 A.

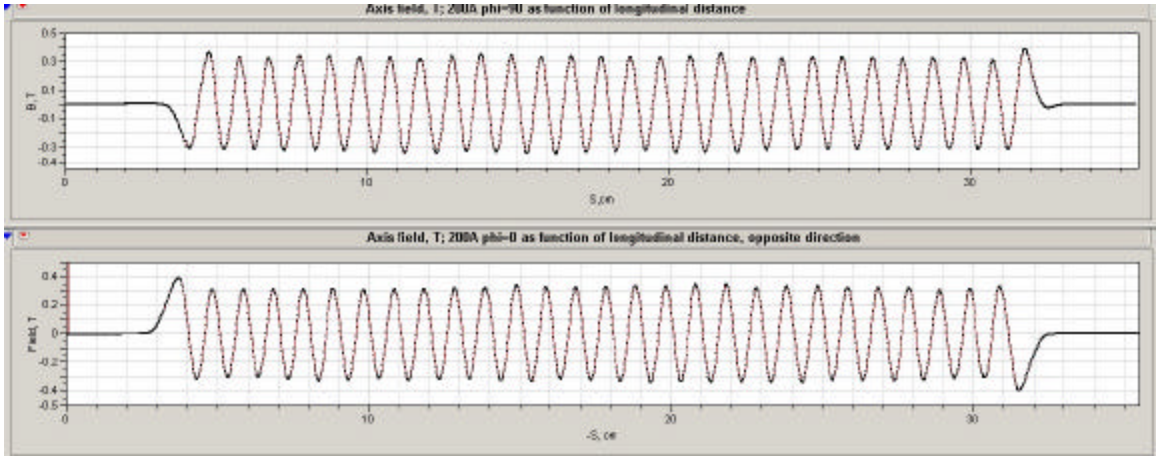

FIGURE 18: Longitudinal field profile measured with Hall probe at Cornell. K=0.33 as required.

Calculation of capturing efficiency is going with numerical code CONVER and by trajectory tracking. Post target hardware –RF, spin rotators. For spin rotator we are considering single line scheme with reversible magnetic field.

CONCLUSIONS

Undulator scheme is preferable for positron production at all times. It is not important—polarized positrons required or not.

Cornell has experience in positron collection optics design. Recent innovations allow collection of 100 mA/ min in CESR ring (perimeter=768m). And this is after acceleration in synchrotron with its inevitable losses.

Fabrication of full scale 4 m—long module allows to test it with real beam and get real cost estimation. So far a sum of 200k$ per fully equipped 4-m module (PS, movers, pickups, trim coils/lenses) looks like a realistic number. About 50 modules required, coming to the cost ~10M$ for all undulator.

Schemes for the target, collimator and focusing lens look feasible.